INTERSPEECH 2023
20-24 August 2023, Dublin, Ireland

Coherence Estimation Tracks Auditory Attention in Listeners with Hearing Impairment

Oskar Keding[1], *Emina Alickovic*[2,3], *Martin A. Skoglund*[2,3], *Maria Sandsten*[1]

[1]Centre for Mathematical Sciences, Lund University
[2]Automatic Control, Department of Electrical Engineering, Linköping University
[3]Eriksholm Research Centre, Snekkersten, Denmark

{firstname.lastname}@matstat.lu.se, {firstname.lastname}@liu.se,
{eali,mnsk}@eriksholm.com

Abstract

Coherence estimation between speech envelope and electroencephalography (EEG) is a proven method in neural speech tracking. This paper proposes an improved coherence estimation algorithm which utilises phase sensitive multitaper cross-spectral estimation. Estimated EEG coherence differences between attended and ignored speech envelopes for a hearing impaired (HI) population are evaluated and compared. Testing was made on 31 HI subjects and showed significant coherence differences for grand averages over the delta, theta, and alpha EEG bands. Significance of increased coherence for attended speech was stronger for the new method compared to the traditional method. The new method of estimating EEG coherence, improves statistical detection performance and enables more rigorous data-based hypothesis-testing results.

Index Terms: Selective Auditory Attention, EEG, Coherence Estimation, Multitaper, Neural Speech Tracking.

1. Introduction

In a number of real-life listening scenarios, a listener has to 'track' and understand an attended speech in the presence of multiple competing talkers. This constitutes the cocktail party problem [1], effectively solved by listeners with normal hearing (NH) in everyday life, and less effectively in listeners with hearing impairment (HI) [2]. For this reason, algorithms to measure neural tracking (NT) of natural running speech from electroencephalography (EEG) [3] have been developed in order to understand how attention and hearing are related. These algorithms are especially important for HI listeners that are in need of intuitive and adaptive hearing aids (HAs) [4–7]. One practical way to understand how the neural activity tracks speech is by relating the neural responses to the speech signals, for example using linear filters.

Implementation of linear filter estimation assumes the speech as an input signal to the process in the brain and viewing EEG as the output signal [8, 9]. Although there are a plethora of error sources, a transfer function that maps speech features to EEG can then be estimated. This can then be used to decode auditory attention. Success with linear filters, from speech envelopes to recorded EEG signals, has been shown [3,4,6,10,11]. Alternatively, one can use coherence measures [12] to detect linear, or first order, correlation of input speech and output EEG.

One version of coherence estimators is the magnitude squared coherence (MSC) function, defined as the squared cross-spectrum normalised with the auto-spectra of the two channels. Finding reliable estimates of the MSC are important in many applications, such as signal detection, frequency function estimation, time delay estimation and system identification [13]. MSC has been studied for many years where the Welch method and the Thomson multitapers commonly are applied [14–16].

Previously, Viswanathan et al. [17] showed statistically significant differences in coherence values between attended and ignored speech stream for NH listeners. Using a Thomson multitaper based coherence estimator over multiple data segments, they showed strong statistical significance for attended and ignored speech difference, in the delta, theta and alpha EEG spectral bands. As the amount of noise in EEG data is substantially large, the coherence estimates are often very small between the input speech envelopes and EEG, which sometimes makes detection of coherence to become difficult [18, 19].

This work employs a similar coherence estimation algorithm as in [17], with the difference that the proposed method utilises phase information in the tapers. As such, better coherence detection is obtained, improving on the ability to distinguish differences in attended to ignored speech for HI listeners. Simulations are presented to illustrate the difference in performance of the coherence estimation method choices.

2. Research Data

2.1. Study Design

The experimental protocol was reviewed and approved by the Science Ethics Committee for the Capital Region of Denmark (journal no. H20028542). The EEG data utilized in this paper have been used for different type of analyses in [7].

2.1.1. Participants

Participants comprised 31 experienced HA users with mild to moderately severe sensorineural hearing loss (mean age 65.6). All participants were native Danish speakers, with no history of neurological disorders, dyslexia, or diabetes mellitus.

2.1.2. Stimuli and Recording

Stimuli were routed through a sound card (RME Hammerfall DSP multiface II, Audio AG, Germany) and were played via 6 loudspeakers (Genelec 8040A; Genelec Oy, Finland) at a $44{,}1\,\mathrm{kHz}$ sampling rate. Loudspeakers were positioned at $\pm 30^\circ$ (T1-T2), $\pm 112.5^\circ$ (B1-B2) and $\pm 157.5^\circ$ (B3-B4) azimuth, see Figure 1a. Attended and ignored stimuli (T1-T2) were presented at $73\,\mathrm{dB}$ SPL each. Background noise (B1-B4) was played at $70\,\mathrm{dB}$ SPL through 4 loudspeakers, with a mix of 4 talkers in each loudspeaker. The stimuli comprised 84 $\sim 33\,\mathrm{s}$-long segments (trials) read by the same male and female talker. Four trials were used for subject training and 80 trials used for analysis. Each trial comprised a short period of silence, $5\,\mathrm{s}$ of

Thanks to the ELLIIT strategic research programme for funding.

10.21437/Interspeech.2023-633

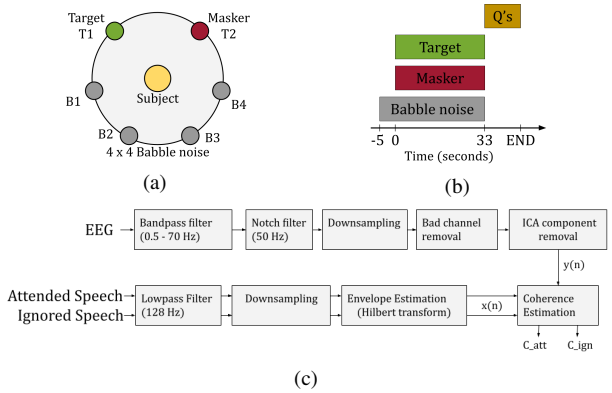

Figure 1: *Schematic illustration of (a) the experimental set-up, (b) trial paradigm design and (c) pre-processing pipeline.*

background noise, 33 s of simultaneous stimuli from all speakers followed by a two-choice question about the content of the attended speech, as illustrated in Figure 1b. EEG data were acquired at a sampling rate of 1024 Hz with a BioSemi ActiveTwo 64-channel EEG recording system in 10-20 layout. A more detailed description of the experimental design is provided in [6, 7].

2.2. EEG Preprocessing

EEG signals were referenced to the average of mastoid channels, bandpass filtered between 0.5 and 70 Hz and notch filtered at 50 Hz to remove line noise. EEG was downsampled to 256 Hz, to avoid unnecessary temporal computation. Bad channels, on average 0.87 channels per subject, were removed and interpolated from remaining channels. Independent component analysis [20, 21] was performed, manually removing clear noise components such as eye artefacts, muscle activity, heart-beats and single channel noise, with an average of 17 components removed per subject.

Speech signals of the attended and ignored talkers were low-pass filtered at 128 Hz and downsampled to 256 Hz, and subsequently envelopes of the speech were calculated as the absolute value of the analytical version of the speech signals. The pre-processing steps are summarised in Figure 1c.

3. Coherence Estimation

The measure of spectral coherence is common for detecting and analysing linear systems, i.e., systems where a sampled output signal $y(n)$ is a linear filtering of an input signal $x(n)$. The measure can have various forms, here as the MSC defined as

$$C_{xy}(f) = \frac{\hat{S}_{xy}(f)^2}{\hat{S}_{xx}(f)\ \hat{S}_{yy}(f)} \tag{1}$$

The estimated auto-spectra $\hat{S}_{xx}(f)$ and $\hat{S}_{yy}(f)$ are calculated as

$$\hat{S}_{xx}(f) = \frac{1}{KL}\sum_{k=1}^{K}\sum_{l=1}^{L} X_{k,l}(f)X_{k,l}(f)^* \tag{2}$$

$$\hat{S}_{yy}(f) = \frac{1}{KL}\sum_{k=1}^{K}\sum_{l=1}^{L} Y_{k,l}(f)Y_{k,l}(f)^* \tag{3}$$

where $X_{k,l}$ and $Y_{k,l}$ are the discrete Fourier transforms (DFT) of data segment l tapered by the k:th window and $*$ is defining complex conjugate. The windows are selected by design to reduce the variance of the spectral estimator. In the present study, Thomsons method is used, as these multitapers maximise the narrowband power of the spectral estimate as well as reduce estimation variance [16].

Traditionally, in the field, the multitaper cross-spectrum in the numerator of Eq. (1) has been estimated as

$$\hat{S}_{xy}^{trad}(f) = \frac{1}{KL}\sum_{k=1}^{K}|\sum_{l=1}^{L} X_{k,l}(f)Y_{k,l}(f)^*| \tag{4}$$

with the absolute value inside the sum of the multitaper cross-spectra. In this contribution, we instead propose an estimate according to

$$\hat{S}_{xy}^{new}(f) = \frac{1}{KL}|\sum_{k=1}^{K}\sum_{l=1}^{L} X_{k,l}(f)Y_{k,l}(f)^*| \tag{5}$$

where the absolute value now is outside the multitaper cross-spectrum. The MSC method utilising cross-spectra as Eq. (4) is referred to as the traditional method where the proposed technique in Eq. (5) is named the new method. MSC estimation essentially sums the complex cross-spectra over tapers and data segments and then normalises, which magnifies components that are phase-locked between the sub-estimates and strikes out the components that are not. The traditional method removes the phase component in each cross-spectrum before averaging together where the new method actually takes the phase into account, thereby utilising all available information.

4. Simulation Evaluation

In this section the new method will be compared to the traditional method for simulated signals. Two evaluations are made, where the simulation design and parameters are chosen to closely relate to the application of the use of the MSC in selective auditory attention tasks. The first evaluation compares detection of coherence, for two cases: coupling and no-coupling. The second evaluation illustrates a shifting phenomenon of the coherence peaks for additive $1/f$-noise, often used as a simulated low-frequency component of EEG [22].

4.1. Signal Detection Comparison

MSC estimates are generated for coupling versus no-coupling, where the coupling case is when a signal is present both in input and output signal. The no-coupling case is when the signal is present in the input signal but not in the output signal. All input and output signals are perturbed by uncorrelated additive white noise. The distributions of MSC estimates are evaluated for both the new method and the traditional method, and both coupling scenarios.

The simulation entails generating the input signal $s(n)$ as unitary-powered white noise band-passed in the region 8-10 Hz. The input is disturbed by white noise, $e_x(n)$, of varying standard deviation $\sigma_x \in [2, 5, 10]$, giving $x(n) = s(n) + \sigma_x e_x(n)$. The outputs for the coupling and no-coupling scenarios are defined as $y(n) = s(n) + \sigma_y e_y(n)$ and, $y(n) = \sigma_y e_y(n)$ respectively, where $e_y(n)$ is white uncorrelated noise of different standard deviations $\sigma_y \in [0, 0.1, 0.2, ..., 10]$. For each MSC estimate 33 s of data is used with $L = 33$ and segment length 256. The sampling frequency is $f_s = 256$, the FFT-length is 256 and the number of multitapers is $K = 10$. Simulations were performed 10000 times, and the two MSC measures were

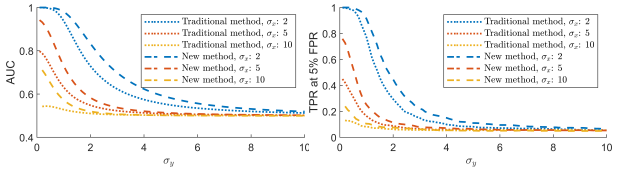

(a) (b)

Figure 2: *(a) Area under curve for both method in our simulation. (b) True positive rate at 5% false positive rate for both method in our simulation.*

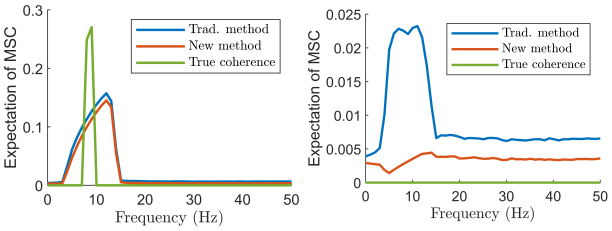

(a) (b)

Figure 3: *Expectation of coherence estimation for bandpass filtered white noise in the presence of pink noise in (a) coupling and (b) no-coupling scenario. One can clearly see that the spectral position of the peak is shifted in a positive direction in the coupling case in the left figure. The right figure shows the biases for the methods of interest in the no-coupling case, where there should ideally be no peak.*

estimated using the mean value of the frequency bins entailed in the signal band 8–10 Hz.

A receiver operating characteristic (ROC) curve for the simulated empirical distributions of MSC estimates of coupling and no-coupling scenarios. The area under curve (AUC) is shown in Figure 2a and a second measure, the true positive rate (TPR) at the 5% false positive rate (FPR) is presented in 2b. The two measures of detection performance are very consistent with each other, showing similar trajectories over noise power levels. However, the two methods differ in performances. Firstly, a consistent improvement over all combinations of noise powers σ_x and σ_y utilising the new method compared to the traditional method can be observed. Secondly, an observation can be made that the difference between the two methods is larger when there are significant levels of noise in both channels compared to when a clean observation of the input signal can be made.

4.2. The Effect of EEG-Like Pink Noise

In reality, EEG data do not conform to the noise assumption of the simulation presented in previous section. Output noise in this case is not well-defined white noise, but consists of other cortical processes, conduction noise and measurement noise from a multitude of sources. One effect that is observable when changing the nature of the noise processes obstructing the system, is shown by changing the noise colour to an EEG-like $1/f$-noise (pink noise).

In Figure 3, the estimated coherence expectation of a coupling (left) and no-coupling scenario (right) is shown. An identical simulation as in the previous section was performed, with two differences. The first difference is that $x(n) = s(n)$, without noise disturbance. The second difference is that $e_y(n)$ now is 1/f-noise to emulate the observed low-frequency noise of EEG data. The pink noise was simulated by Fourier transforming generated white noise, multiplying with the $1/f$-spectra, then inverse transforming and ensuring zero mean and standard deviation one. The estimated MSC expectations for the no-coupling and coupling cases were then evaluated at all positive frequencies. Observable in Figure 3, the peaks of the coherence do not lie in the true spectral band of the signal but are instead shifted to higher frequencies, which is due to spectral leakage and the slanted power spectrum of noise. This risks interpretation errors in identifying spectral locations of components correlated in channels. Accounting for this is beyond the scope of this paper, but worthy of focus in future work. Additionally, one can also see that there is a larger (biased) peak in the coherence spectra in the no-coupling case for the traditional method compared to the new method. The coherence spectra should ideally be flat, which indicates that the new method is preferable to apply.

5. Real Data Evaluation

Coherence between speech envelopes and EEG responses gives a measure of to what extent the cortical responses can be linearly predicted from sound. In the experimental setup described in Section 2.1 one seeks to know whether it is possible to see significant differences in speech-EEG coherences when the speech stream is attended $x_{att}(n)$ compared to when it is ignored $x_{ign}(n)$ (in a positive direction for attended speech), given the set of all data spanning trials and subjects. For each trial, MSC is estimated with the same parameters as in the simulation of section 4.1, but with twice the FFT-length. Speech-EEG coherence estimates are made for multiple EEG frequency bands, taking the mean over all channels as well as over the delta (1 - 4 Hz), theta (4 - 8 Hz), alpha (8 - 12 Hz), beta (12 - 30) and gamma band (32 - 128 Hz) respectively. A hypothesis test can be constructed to estimate this difference. In order for the coherence, averaged in a frequency band B, between attended speech envelopes (C^B_{att}) and EEG to be larger than for the unattended speech envelopes (C^B_{ign}) and EEG the following inequality should be shown for the stochastic variables $E[\hat{C}^B_{att}] > E[\hat{C}^B_{ign}]$. An equivalent statement is to look at $E[\hat{D}] = E[\hat{C}^B_{att} - \hat{C}^B_{ign}]$ and showing this to be positive. This analysis can be done for each EEG channel separately, or for the average coherence over all EEG channels compared to speech envelopes. Associated hypotheses for the test can be formed as

H_0: Attended speech coherence estimates are equal or smaller compared to ignored speech coherence estimates, $E[\hat{D}] \leq 0$.

H_1: Attended speech coherence estimates are larger than ignored speech coherence estimates, $E[\hat{D}] > 0$.

A null distribution of D is approximated through bootstrap sampling by firstly randomising the sign of D for each trial and subject and secondly taking the mean over all trials and subjects [17, 23]. This procedure is repeated 500 000 times to approximate the underlying distribution of $D^B_{H_0}$. The p-values of each sampled $\hat{D}^B_{H_0}$ estimate are calculated through the approximated null distributions. The p-value comparison is proofed against multiple comparisons by using Boneferroni correction [24].

Figure 4 shows the grand average of coherence estimates over all channels, experiment trials and subjects, in an estimated 95% confidence interval, for attended and ignored speech envelopes. Overall, for lower frequencies the coupling is stronger between attended speech envelopes and EEG responses, compared to the ignored speech, using both methods. However, the

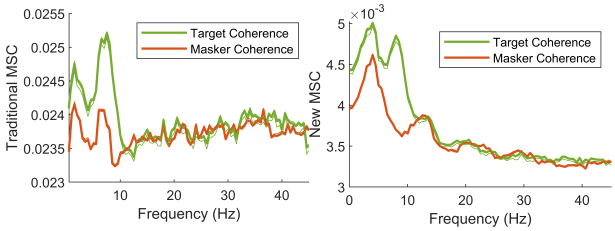

Figure 4: *The grand average coherence estimates, over EEG channels, trials and subjects, calculated with (a) the traditional method and (b) the new method.*

new method is sustantially lower, perhaps indicating a bias effect in the estimate using the traditional method.

Coherence was also estimated, taking the mean over all channels, and over EEG bands. The null hypothesis was tested for observed coherence difference between attended and ignored speech envelope coherence, as described in the beginning of section 5. This resulted in a series of p-values for each EEG-band, shown in Figure 5 for both the traditional method and new method. First, for HI listeners, very similar conclusions regarding for which EEG-bands the rejection of the null hypothesis can be made, compared to an NH population, for example in [17]. The delta, theta and alpha band coherence estimators show a significant difference in attended and ignored coherence, with a 95% (Boneferroni corrected) confidence.

Both methods capture consistent patterns of significant EEG bands. However, the p-values are consistently lower for the new method compared to the traditional method. These results reflect the behaviour similar to the simulation results of section 4.1. In this case, both methods are good enough for reliable statistical conclusions. However, one would potentially need less trials with use of the new method to make conclusions about the coherence difference.

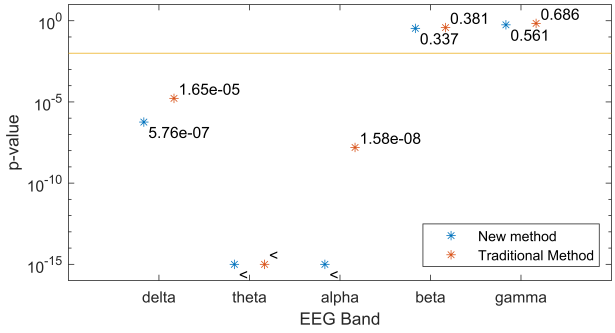

Figure 5: *Given the null hypothesis of $C^B_{att} \leq C^B_{ign}$, the figure shows p-values of measured grand average coherence over all trials and subjects, calculated for each EEG band. Coherence estimation using the new method and using the traditional method is shown in blue and red respectively. The sign $<$ denotes p-values estimated lower than the limit 10^{-15}.*

A similar p-value test is made for each frequency bin of the coherence estimates of the new method, instead of a mean of entire EEG-bands, for which the p-values are shown in Figure 6. Although the Bonferroni correction is a lot more stringent and a variance reducing mean is not performed before hypothesis testing, certain bins still show significant differences in attended and ignored speech coherence. These bins range 5-10 Hz.

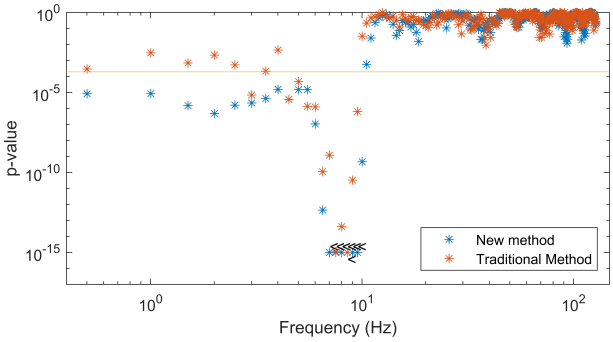

Figure 6: *Given the null hypothesis of $C^B_{att} \leq C^B_{ign}$, the figure shows p-values of measured grand average coherence over all trials and subjects, calculated for each frequency. Coherence estimation using new method and using the traditional method is shown in blue and red respectively. The sign $<$ denotes p-values estimated lower than the limit 10^{-15} and is above the data point for blue stars and below for red.*

Lastly, to identify the important channels for EEG-based speech tracking, a hypothesis test was also performed for each channel, averaging the coherence in the delta, theta, and alpha band. The significant channels can be seen in Figure 7, which gives possibility to redo steps in previous coherence p-value testing a better optimal frequency identification. One should note that significant channels may contain redundant information compared to each other, which means all of them may not be needed in a neural speech tracking application.

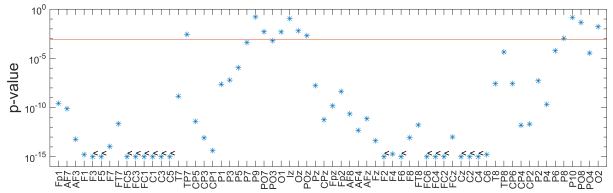

Figure 7: *P-values of mean coherence difference over channels, of which were made averaging frequency bins within the delta, theta and alpha band. The sign $<$ denotes p-values estimated lower than the limit 10^{-15}.*

6. Conclusions

The new method of estimating coherence proposed in this study, utilising all available phase-information, has been shown to improve statistical detection ability of coherence through simulation. Investigating a real data application within auditory attention tracking, coherence estimates between speech envelope and EEG has proven to significantly differ between using attended speech envelopes and ignored speech envelopes as inputs, and the new method has an increased estimated difference compared to the traditional method. Specifically, this was shown for a hearing impaired population of 31 subjects. Statistical testing showed significant differences for the delta, theta, and alpha EEG bands. These results are consistent with previous findings of important EEG bands for a normal hearing population. As a future work, we aim to improve spectral shifting bias in realistic noise scenarios, with the ultimate goal to be able to evaluate and further advance hearing technology.

7. References

[1] E. C. Cherry, "Some Experiments on the Recognition of Speech, with One and with Two Ears," *The Journal of the Acoustical Society of America*, vol. 25, no. 5, pp. 975–979, Sep. 1953. [Online]. Available: http://asa.scitation.org/doi/10.1121/1.1907229

[2] B. G. Shinn-Cunningham and V. Best, "Selective attention in normal and impaired hearing," *Trends Amplif.*, vol. 12, no. 4, pp. 283–299, 2008.

[3] J. A. O'sullivan, A. J. Power, N. Mesgarani, S. Rajaram, J. J. Foxe, B. G. Shinn-Cunningham, M. Slaney, S. A. Shamma, and E. C. Lalor, "Attentional selection in a cocktail party environment can be decoded from single-trial EEG," *Cerebral cortex*, vol. 25, no. 7, pp. 1697–1706, 2015.

[4] E. Alickovic, T. Lunner, D. Wendt, L. Fiedler, R. Hietkamp, E. H. N. Ng, and C. Graversen, "Neural representation enhanced for speech and reduced for background noise with a hearing aid noise reduction scheme during a selective attention task," *Frontiers in neuroscience*, vol. 14, p. 846, 2020.

[5] T. Lunner, E. Alickovic, C. Graversen, E. H. N. Ng, D. Wendt, and G. Keidser, "Three new outcome measures that tap into cognitive processes required for real-life communication," *Ear and hearing*, vol. 41, no. Suppl 1, p. 39S, 2020.

[6] E. Alickovic, E. H. N. Ng, L. Fiedler, S. Santurette, H. Innes-Brown, and C. Graversen, "Effects of Hearing Aid Noise Reduction on Early and Late Cortical Representations of Competing Talkers in Noise," *Frontiers in Neuroscience*, vol. 15, p. 636060, Mar. 2021. [Online]. Available: https://www.frontiersin.org/articles/10.3389/fnins.2021.636060/full

[7] A. H. Andersen, S. Santurette, M. S. Pedersen, E. Alickovic, L. Fiedler, J. Jensen, and T. Behrens, "Creating clarity in noisy environments by using deep learning in hearing aids," in *Seminars in Hearing*, vol. 42, no. 03. Thieme Medical Publishers, Inc., 2021, pp. 260–281.

[8] E. Alickovic, T. Lunner, F. Gustafsson, and L. Ljung, "A tutorial on auditory attention identification methods," *Frontiers in neuroscience*, p. 153, 2019.

[9] S. Geirnaert, S. Vandecappelle, E. Alickovic, A. de Cheveigne, E. Lalor, B. T. Meyer, S. Miran, T. Francart, and A. Bertrand, "Electroencephalography-based auditory attention decoding: Toward neurosteered hearing devices," *IEEE Signal Processing Magazine*, vol. 38, no. 4, pp. 89–102, 2021.

[10] B. Mirkovic, M. G. Bleichner, M. De Vos, and S. Debener, "Target speaker detection with concealed EEG around the ear," *Frontiers in neuroscience*, vol. 10, p. 349, 2016.

[11] L. Fiedler, M. Wöstmann, C. Graversen, A. Brandmeyer, T. Lunner, and J. Obleser, "Single-channel in-ear-EEG detects the focus of auditory attention to concurrent tone streams and mixed speech," *Journal of neural engineering*, vol. 14, no. 3, p. 036020, 2017.

[12] R. A. Dobie and M. J. Wilson, "Analysis of auditory evoked potentials by magnitude-squared coherence," *Ear and hearing*, vol. 10, no. 1, pp. 2–13, 1989.

[13] G. C. Carter, "Coherence and time delay estimation," *Proc. of the IEEE*, vol. 75, no. 2, pp. 236–255, Feb 1987.

[14] S. Y. Wang, "Exact confidence interval for magnitude-squared coherence estimates," *IEEE Signal Processing Letters*, vol. 11, no. 3, pp. 326–329, March 2004.

[15] G. D. Brushe and J. R. Waller, "On the computation of an averaged coherence function," *Digital Signal Processing*, vol. 11, no. 2, pp. 111–119, 2001.

[16] D. J. Thomson, "Spectrum Estimation and Harmonic Analysis," *Proceedings of the IEEE*, vol. 70, no. 9, pp. 1055–1096, 1982.

[17] V. Viswanathan, H. M. Bharadwaj, and B. G. Shinn-Cunningham, "Electroencephalographic Signatures of the Neural Representation of Speech during Selective Attention," *eneuro*, vol. 6, no. 5, pp. ENEURO.0057–19.2019, Sep. 2019. [Online]. Available: https://www.eneuro.org/lookup/doi/10.1523/ENEURO.0057-19.2019

[18] F. Destoky, M. Philippe, J. Bertels, M. Verhasselt, N. Coquelet, M. Vander Ghinst, V. Wens, X. De Tiège, and M. Bourguignon, "Comparing the potential of MEG and EEG to uncover brain tracking of speech temporal envelope," *Neuroimage*, vol. 184, pp. 201–213, 2019.

[19] Y.-P. Chen, F. Schmidt, A. Keitel, S. Rösch, A. Hauswald, and N. Weisz, "Speech intelligibility changes the temporal evolution of neural speech tracking," *NeuroImage*, p. 119894, 2023.

[20] A. J. Bell and T. J. Sejnowski, "An information-maximization approach to blind separation and blind deconvolution," *Neural computation*, vol. 7, no. 6, pp. 1129–1159, 1995.

[21] A. Delorme and S. Makeig, "EEGLAB: an open source toolbox for analysis of single-trial EEG dynamics including independent component analysis," *Journal of neuroscience methods*, vol. 134, no. 1, pp. 9–21, 2004.

[22] E. Barzegaran, S. Bosse, P. J. Kohler, and A. M. Norcia, "EEGSourceSim: A framework for realistic simulation of EEG scalp data using MRI-based forward models and biologically plausible signals and noise." *Journal of Neuroscience Methods*, vol. 328, 2019.

[23] N. Te and H. Ap, "Nonparametric permutation tests for functional neuroimaging: a primer with examples," *Human brain mapping*, vol. 15, no. 1, Jan. 2002, publisher: Hum Brain Mapp. [Online]. Available: https://pubmed.ncbi.nlm.nih.gov/11747097/

[24] O. J. Dunn, "Multiple comparisons among means," *Journal of the American Statistical Association*, vol. 56, no. 293, pp. 52–64, 1961.